BENTHAM OPEN

CrossMark

The Open Civil Engineering Journal

RESEARCH ARTICLE

Nonlinear Numerical Analyses of a Fabricated Connection of Concrete-Filled Steel Column to Steel Beam Under Low-Reversed Cyclic Loading

Chunyi Cui[1,3,*], Kun Meng[1], Yan Kong[1], Yannian Zhang[2] and Wenxin Zuo[3]

[1]*Department of Civil Engineering, Dalian Maritime University, Dalian 116026, China*
[2]*School of Civil Engineering, Shenyang Jianzhu University, Shenyang 110168, China*
[3]*School of Civil and Mechanical Engineering, University of Birmingham, Birmingham, B15 2TT, United Kingdom*

Abstract:

Introduction:

Based on FEM program ABAQUS, three-dimensional numerical models of a fabricated connection of concrete-filled steel column to steel beam under low-reversed cyclic loading were established by considering both nonlinearity of material and geometry. Effects of stiffen ring plate, axial compression ratio and backing plate on the hysteresis curves, skeleton curves, ductility coefficient and energy dissipation coefficient were analyzed respectively.

Methods:

Furthermore, parametric analyses with comparison were also conducted to discuss the mechanical characteristics and damage mechanism of the fabricated connection.

Results:

The results show that there are clear stress concentrations near the area of bolt holes in beam flange. The increase in width of ring plate and the shape change of ring plate from square to circle can both improve the ductility and the characteristics of hysteretic behavior. Besides, the backing plates have positive effects on the hysteretic characteristics, ductility and energy dissipation of the CFST column connections. Oppositely, the increase in axial compression ratio contributes negatively to both the bearing capacity and deformation performance of the connection specimens.

Conclucion:

It can be concluded that the fabricated connection displays good working performance relating to hysteretic characteristics, energy dissipation and ductility, which can be hopefully applied and provide reference to engineering practice.

Keywords: Numerical analysis, Cyclic loading, Ductility, Hysteretic behavior, Energy dissipation, Connection.
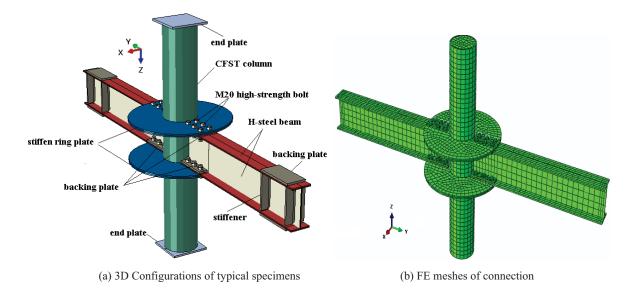
1. INTRODUCTION

In the last thirty years, concrete-filled steel tubular (CFST) columns were widely employed as compression materials in high-rise buildings, long-span bridges, and underground structures due to the advantages of good performance, construction convenience, fine fire resistance as well as low construction cost [1, 2]. CFST columns are known to increase the strength and stiffness of the section by confining the concrete panel in the steel tube. With the application of CFST columns into engineering practices, different types of connections have been developed to

* Address correspondence to this author at the Department of Civil Engineering, Dalian Maritime University, Dalian 116026, China; Tel: +86-15542419801; E-mail: cuichunyi@dlmu.edu.cn

connect flange beams to steel tube columns [3, 4]. According to the "specification for design and construction of a steel pipe concrete structure (CECS28:90)," beam-column connections should be fine and satisfy the design criterion of strong column and weak beam. The corresponding modes of load transfer and construction technology are two key aspects of connection design, as emphasized by Ricles and Gregory *et al.* [5, 6]. Researchers have conducted many studies on CFST column and beam connections. Numerical analyses are adopted by most researchers in analyzing the deformation capacity of CFST column-beam connections aside from cyclic loading tests.

The seismic performance of concrete-filled steel square tube column connection with H beams was investigated by Morino *et al.* [7]. The ductility and energy dissipation of concrete-filled steel square tubular column connections were discussed [8 - 11]. Moreover, both the characteristics of the stress concentration and plastic hinge in the embedded type of CFST column connections were reported by Beutel *et al.*, Chiew *et al.*, and Li *et al.* [12 - 14]. Based on previous engineering practice and research, the effects of geometric features of connections, axial compression ratio, and other factors on the performance, such as ductility and hysteretic characteristics of CFST column connections were discussed [15 - 20]. However, most presented types of CFST column connections are connected through a welding technique. This may lead to construction inconvenience and frameworks inefficiency, particularly for the complicated and structures. Meanwhile, fabricated beams with the connector of high strength friction grip bolt are promising for designing CFST column connections, which are easily operated and can satisfy the strength requirements in engineering materials. Moreover, research on CFST column connections with assembled beams without welding is limited both in theoretical analysis and experimental investigation.

(a) 3D Configurations of typical specimens   (b) FE meshes of connection

Fig. (1). Computational model of connection.

This work aims to investigate a new type of fabricated connection of concrete-filled steel column to steel beam by developing three-dimensional numerical models of the cross-shaped connection under low-reversed cyclic loading and carrying out parametric analyses to discuss the mechanical characteristics and the damage mechanism of the fabricated connection. Moreover, comparative analyses with experimental results are conducted to analyze the effects of the stiffen ring plate, axial compression ratio, and backing plate on hysteresis curves, skeleton curves, ductility coefficient, and energy dissipation coefficient.

2. MATERIALS AND METHODS

2.1. Numerical Model of the Proposed Connection

The computational model of the connections used in this research is shown in Fig. (**1**), in which both the three-dimensional configurations and the FEM meshes of connection are depicted. The detailed material properties of connections are listed in Table **1**, and the strengths of concrete and steel are determined through tensional coupon tests. Six numerical specimens were developed according to the schedule of specimens listed in Table **2**. Square ring plate

was adopted in the specimen F12D3. The axial force for CFST column was of 5000 kN magnitude and applied through the axis of the steel tube. The cyclic loading according to a quasi-static cyclic displacement pattern was defined in terms of beam end displacement and was applied vertically to the H-beams based on the loading scheme in Fig. (**2**). The loading pattern was applied to each specimen until failure occurred.

Table 1. Mechanical properties of connection materials.

Material	Material class	Young's module (MPa)	Poisson ratio	Yield strength of tension (MPa)	Ultimate strength of tension (MPa)
Concrete	C60	3.6×10^4	0.2	35.738	64.39
Steel	Q345	2.1×10^5	0.24	310	448

Table 2. Dimensional details of specimens.

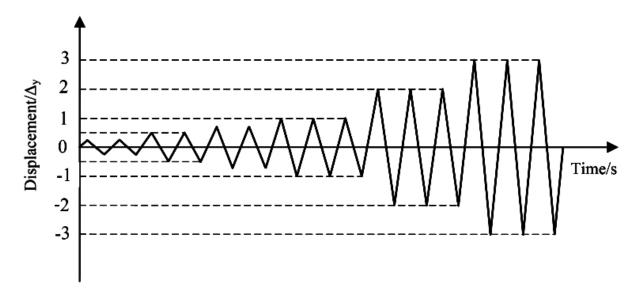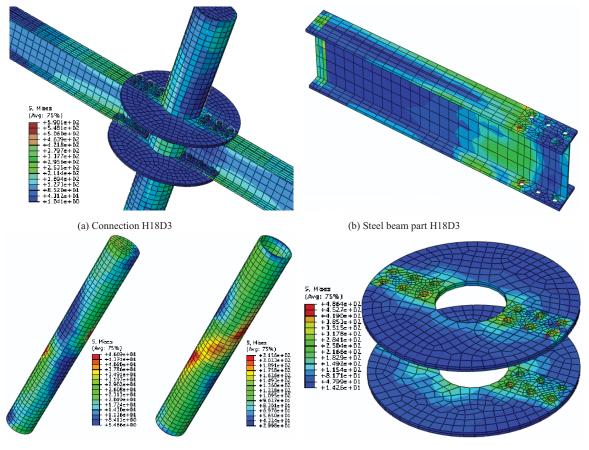| Specimen	Backing plate	Column (mm)		H-beam (mm)		Axial compression ratio	Width of ring plate (mm)
		Cross section	Length	Cross section	Length		
H18D3	with	$\phi180\times8.00$	1250	200×100×8×5.5	2080	0.3	180 (circular)
H18W3	without	$\phi180\times8.00$	1250	200×100×8×5.5	2080	0.3	180 (circular)
H18D6	with	$\phi180\times8.00$	1250	200×100×8×5.5	2080	0.6	180 (circular)
H18W6	without	$\phi180\times8.00$	1250	200×100×8×5.5	2080	0.6	180 (circular)
H12D3	with	$\phi180\times8.00$	1250	200×100×8×5.5	2080	0.3	120 (circular)
F12D3	with	$\phi180\times8.00$	1250	200×100×8×5.5	2080	0.3	127 (square)

Fig. (2). Cyclic loading scheme.

3. NUMERICAL RESULTS AND DISCUSSION

Fig. (**3a-b**) show the distribution of the Mises stress of connection H18D3 when the displacement load equals Δ_y. The stress amplitude in the beam flange is higher than that on the web. This is in accordance with the experimental description [21 - 23], which is measured in connection with the experiments through MTS servo loading system. A plastic zone is far away from the welding area due to the installation of the stiffen plate on the steel beam, and this can prevent the beam from rupture at the welding location. However, welding quality should be given importance during fabrication because the welding location still has stress concentration. The distribution of the Mises stresses of the CFST column in connection with H18D3 when the displacement load equals $3\Delta_y$ is shown in Fig. (**3c**). As shown, an X pattern of stress concentration exists near the connection intersection. Moreover, the distribution of the Mises stress of

the stiffen plate in connection with H18W6 when the displacement load equals $3\Delta_y$ is shown in Fig. (**3d**). As shown, the stress variation along the axis of the steel beam is significant, and significant stress concentration exists near the contact area between the stiffen plate and the steel beam. Moreover, the improvement of the stiffen plate on the distribution of the forces of the connection, *i.e.*, the existence of stiffen plate is helpful for the effective transfer of the load from the beam end to the CFST column.

(a) Connection H18D3

(b) Steel beam part H18D3

(c) Concrete and steel tube of connection H18W3

(d) Stiffen ring plate of connection H18W6\

Fig. (3). Contours of the Mises stress of the connection.

The comparisons of the P-Δ hysteretic curves between experimental data and computational results are shown in Fig. (**4**). The hysteretic characteristics of each specimen become more robust with the cyclic increase of displacements, indicating the fine deformation performance of the presented connections. Moreover, the increase in the width of the ring plate and the installation of the backing plate contribute positively to the bearing capacity of the connection specimens. For the idealization of the numerical model, without considering the initial imperfection of specimens due to fabrication, the hysteretic curves from the numerical results above are more regular than those from the experiments.

Fig. (**5**) shows the comparisons of the P-Δ skeleton curves between the experimental data and the computational results. Moreover, the increase in the width of the ring plate and the installation of the backing plate contribute positively to the bearing capacity of the connection specimens. Thus, the specimen with the square ring plate presents higher ultimate and failure loads than the specimen with the circular ring plates. Moreover, all specimens do not show significant degradation of stiffness and strength when loading reaches the ultimate state. That is, the working performance of this type of connection is good.
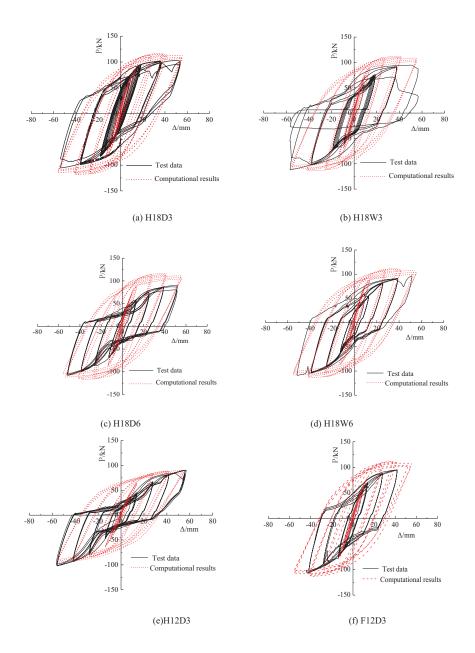
Fig. (4). Comparisons of the P-Δ hysteretic curves between the experimental data and the computational results.

The comparisons of the typical index, including yield displacement, yield load, ultimate displacement, and ultimate load between experimental data, and computational results are listed in Table **3**. Errors toward all typical indexes are minimal and within the acceptable scale. Given the idealization of numerical models without considering the imperfection of fabrication, the index errors of the yield state are less than those of the ultimate state. Integration of the comparisons of ductility coefficient and energy dissipation coefficient between the experimental data and the computational results are listed in Tables **4** and **5**, which indicates that the connection presents good ductility and energy dissipation. All relating indexes satisfy the requirements of the building seismic code. Furthermore, all the index errors of the ductility coefficient and the energy dissipation coefficient between the experimental data and the computational results are minimal and within the acceptable scale.
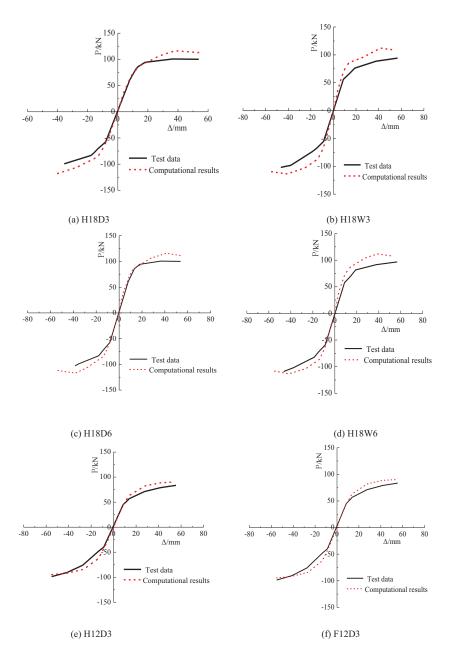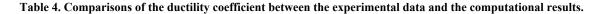
(a) H18D3

(b) H18W3

(c) H18D6

(d) H18W6

(e) H12D3

(f) F12D3

Fig. (5). Comparisons of the P-Δskeleton curves between the experimental data and the computational results.

Table 3. Comparisons of the typical index between the experimental data and the computational results.

Specimen	Yield displacement (mm)			Yield load (kN)			Ultimate displacement (mm)			Ultimate load (kN)		
	Test data	Numerical results	Error	Test data	Numerical results	Error	Test data	Numerical results	Error	Test data	Numerical results	Error
H18D3	17.92	15.2	15%	92.71	89.75	3.2%	58.33	55.04	5.6%	99.84	112.59	13%
H18W3	18.28	15.25	17%	73.77	87.54	19%	59.43	53.55	9.9%	92.7	108.23	16%
H18D6	16.98	13.34	21%	93.69	83.11	11%	54.52	53.87	1.2%	100.57	111.11	10%
H18W6	16.87	15.57	7.7%	75.98	88.28	16%	54.65	53.55	2.0%	95.66	107.36	12%
H12D3	14.76	13.65	7.5%	59.02	61.97	4.7%	59.49	54.03	8.7%	83.11	90.21	8.5%
F12D3	13.92	13.65	1.9%	84.59	76.72	9.3%	48.62	55.66	15%	108.69	107.61	1.0%

Table 4. Comparisons of the ductility coefficient between the experimental data and the computational results.

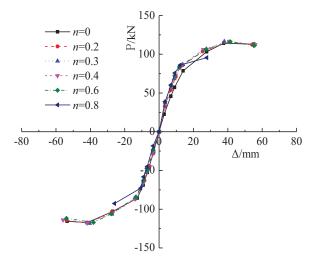| Specimen	Displacement ductility coefficient		Error
	Test data	Numerical results	
H18D3	3.27	3.62	10.09%
H18W3	3.25	3.51	8.00%
H18D6	3.21	4.04	26.85%
H18W6	3.24	3.44	6.17%
H12D3	4.03	3.96	8.44%
F12D3	3.49	4.08	16.91%

Fig. (6). P-Δ skeleton curves under different compression ratios.

Based on the comparative analyses between the numerical results and the experimental data, further parametric analyses must be conducted using numerical extrapolation. The parameters are changed according to the specimen case H18D3.

Table 5. Comparisons of the energy dissipation coefficient between the experimental data and the computational results.

Specimen	Displacement ductility coefficient		Error
	Test data	Numerical results	
H18D3	2.2149	2.4053	8.596%
H18W3	1.9187	2.0486	6.771%
H18D6	1.7571	1.8331	4.325%
H18W6	1.752	1.8522	5.719%
H12D3	1.6148	1.6613	2.88%
F12D3	1.5106	1.6196	7.216%

P-Δ skeleton curves under different compression ratio *n* are shown in Fig. (**6**). The increase of axial compression ratio has negative effects on the bearing capacity and the deformation performance of the connection specimens in accordance with what is displayed in the hysteretic curves above. Fig. (**7**) shows the P-Δ skeleton curves under different concrete strength. As shown, the working performance of the connection becomes worse when the steel tube has no concrete. That is, the existence of core concrete can significantly prevent the steel tube from buckling. Moreover, P-Δ skeleton curves under different tube thickness *t* are shown in Fig. (**8**). The bearing capacity increases with the increase of tube thickness. The influence of the tube thickness on the bearing capacity becomes negligible when the tube thickness reaches 8 mm.
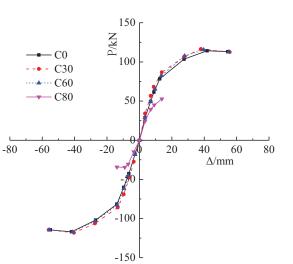
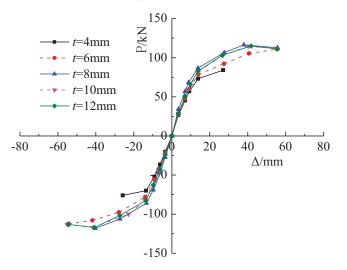**Fig. (7).** P-Δ skeleton curves under different concrete strength.

Fig. (8). P-Δ skeleton curves under different tube thickness.

CONCLUSION

The present work investigated a new type of fabricated connection of concrete-filled steel column to a steel beam by developing three-dimensional numerical models of the cross-shaped connection under low-reversed cyclic loading. Parametric and comparative analyses with experimental results are also performed to discuss the mechanical characteristics and the damage mechanism. The fabricated connection is studied, and several conclusions are drawn, as follows:

1. Clear stress concentrations exist near the area of the bolt holes and near the area of the beam flange for the given connection specimens. The corresponding constructional measures and installations with good quality should be given importance. The presented CFST column connection is of construction convenience and fine deformation performance compared with the CFST column connected through the welding technique and can satisfy the strength requirements as well.
2. The increase of the width of the ring plate and the shape of the ring plate changing from a square to a circle can significantly improve the ductility and the characteristics of the hysteretic behavior of connection. The specimen with the square ring plate is of better deformation performance but lower bearing capacity than the ones with circular ring plates.
3. The backing plates positively affect the hysteretic characteristics, ductility, and energy dissipation of the CFST column connections. They can be installed in the application to lessen cost and for construction convenience.

However, the increase of axial compression ratio negatively affects the bearing capacity and deformation performance of the connection specimens.

4. For the idealization of the numerical model, without considering the initial imperfection of specimens due to fabrication, the numerical results have minor differences from the experimental data but within acceptable errors. Further improvement and optimization of the numerical model must be conducted in future related research. The proposed type of connection can provide reference toward engineering practice and can be applied in future construction projects through further local optimization.

CONSENT FOR PUBLICATION

Not applicable.

CONFLICT OF INTEREST

The authors declare no conflict of interest, financial or otherwise.

ACKNOWLEDGEMENTS

REFERENCES

[1]   D. Martin, O. Shear, and Q. Russell, "Bridge design of circular thin-walled concrete filled steel tubes", *J. Struct. Eng.,* vol. 126, no. 11, pp. 725-758, 2012.

[2]   K.J. Shin, Y.J. Kim, Y.S. Oh, and T.S. Moon, "Behavior of welded CFT column to H-beam connections with external stiffeners", *Eng. Struct.,* vol. 26, pp. 1877-1887, 2004.
        [http://dx.doi.org/10.1016/j.engstruct.2004.06.016]

[3]   J.W. Park, S.M. Kang, and S.C. Yang, "Experimental studies of wide flange beam to square concrete-filled tube column joints with stiffening plates around the column", *J. Struct. Eng.,* vol. 131, no. 12, pp. 1866-1876, 2005.
        [http://dx.doi.org/10.1061/(ASCE)0733-9445(2005)131:12(1866)]

[4]   L. Han, *Theory and Practice of Concrete Filled Steel Tubular Structure,* 2nd ed. Science Press: Beijing, 2007.

[5]   J.M. Ricles, S.W. Peng, and L.W. Lu, "Seismic behavior of composite concrete filled steel tube column-wide flange beam moment connections", *J. Struct. Eng.,* vol. 130, no. 2, pp. 233-243, 2004.
        [http://dx.doi.org/10.1061/(ASCE)0733-9445(2004)130:2(223)]

[6]   M. Gregory, W.R. Charles, G. Chad, and K. Yoshihiro, "Brace-beam-column connections for concentrically braced frames with concrete filled tube columns", *J. Struct. Eng.,* vol. 16, pp. 233-243, 2004.

[7]   S. Morino, "Recent developments in hybrid structures in Japan - research, design and construction", *Eng. Struct.,* vol. 20, pp. 336-346, 1998.

[8]   M. Teraoka, Y Kanoh, and S. Sasaki, "Estimation of yield deformation of beams in interior beam-and-column subassemblages", *Trans. Jpn. Concr. Inst.,* vol. 16, pp. 475-482, 1994.

[9]   J.E. France, J.B. Davison, and P.A. Kirby, "Moment-capacity and rotational stiffness of endplate connections to concrete filled tubular columns with flow drilled connectors", *J. Constr. Steel Res.,* vol. 50, pp. 35-48, 1999.
        [http://dx.doi.org/10.1016/S0143-974X(98)00237-5]

[10]   Z.H. Zong, Y.D. Lin, and H.W. Chen, "Quasi-static test on concrete-filled square steel tube column to steel beam connections", *J. Build. Struct.,* vol. 26, no. 1, pp. 77-84, 2005.

[11]   X.J. Zhou, and H. Qu, "Seismic resistance of bolt-weld joint and all-weld joint of concrete filled square steel tube and steel beam under cyclic load", *China Civ. Eng. J.,* vol. 39, no. 1, p. 38, 2006.

[12]   J. Beutel, D. Thambiratnam, and N. Perera, "Cyclic behavior of concrete filled steel tubular column to steel beam connections", *Eng. Struct.,* vol. 24, no. 11, pp. 29-38, 2002.
        [http://dx.doi.org/10.1016/S0141-0296(01)00083-9]

[13]   S.P. Chiew, S.P. Lie, and C.W. Dai, "Moment resistance of steel I-beam to CFT column connections", *J. Struct. Eng.,* vol. 127, no. 10, pp. 1164-1172, 2001.
        [http://dx.doi.org/10.1061/(ASCE)0733-9445(2001)127:10(1164)]

[14]   C.Y. Li, Y.J. Guo, and M.D. Li, "Experimental study on rigidity of concrete filled steel tubular external strengthening ring node", *Ind. Build.,* vol. 36, no. 9, pp. 81-83, 2006.

[15] S.M. Zhang, and D.X. Zhang, "Load-displacement hysteretic curve theory analysis of reinforced concrete column and beam joint", *J. Harbin Univ. Civ. Eng. Archit.,* vol. 34, no. 4, pp. 1-6, 2001.

[16] J. Chen, Z. Wang, and J.X. Yuan, "Research on the stiffness of concrete filled tubular column and steel beam joint with stiffening ring", *J. Build. Struct.,* vol. 25, no. 4, pp. 43-54, 2004.

[17] C.T. Cheng, P.S. Hwang, L.Y. Lu, and L.L. Chung, "Connection behavior of steel beam to concrete-filled circular steel tubes", In: *6th ASCCS Conference,* Los Angeles, 2000, pp. 581-589.

[18] C.H. Kang, K.J. Shin, and Y.S. Oh, "Hysteresis behavior of CFT column to H-beam connections with external T-stiffeners and penetrated element", *Eng. Struct.,* vol. 23, pp. 1194-1201, 2001.
[http://dx.doi.org/10.1016/S0141-0296(00)00119-X]

[19] L.H. Xu, H. Fan, and S.B. Liu, "Experimental studies on aseismic behavior of connection between concrete-filled steel square tubular column and steel beam", *Eng. Mech.,* vol. 25, no. 2, pp. 122-131, 2008.

[20] L.R. Zhang, Z.F. Tang, and M.G. Wang, "Experimental research on concrete filled steel tubular column to steel beam connections using sleeve", *Build. Struct.,* vol. 35, no. 8, pp. 73-84, 2005.

[21] J.F. Zhao, "Study on the mechanical properties of Concrete-Filled Steel Tube Column and Steel-beam Fabricated Joints", M.S. Thesis, Shenyang Jianzhu University, Shenyang, China, 2011.

[22] C.Y. Cui, J.F. Zhao, Y.N. Zhang, and W.X. Zuo, "'Experimental analyses of mechanical performance of CFST column to assembled steel H-beam connections'", *Open Mech. Eng. J.,* vol. 8, pp. 270-278, 2014.
[http://dx.doi.org/10.2174/1874155X01408010270]

[23] C. Cui, K. Yan, and X. Cheng, "Numerical analysis of a new composite connection for an underground structure", *Electron. J. Geotech. Eng.,* vol. 21, pp. 2259-2268, 2016.